Exploiting structural (Maxwell-Wagner) polarization effects for the AC-electrokinetic manipulation of objects and media in cell chips

J. Gimsa* and M. Stubbe**

University of Rostock, Chair for Biophysics, Gertrudenstr. 11A, 18057 Rostock, Germany
*jan.gimsa@uni-rostock.de, **marco.stubbe@uni-rostock.de

ABSTRACT

AC fields induce polarization charges at the structural interfaces inside inhomogeneous media. In suspensions or emulsions of micro and nano objects these structures are introduced by phase boundaries such as biological membranes. Nevertheless, local heating may also introduce "smeared interfaces" into homogeneous electrolytes. Subsequently, the interaction of the polarization charges with the inducing field generates AC-electrokinetic forces. The effects observed depend on the temporal and spatial field properties and the frequency dependence of the dipole moment induced in the objects or volumes. For objects, electroorientation (EO), electrodeformation (ED), dielectrophoresis (DP), electrorotation (ER), field-trapping and travelling wave (TW) DP are well investigated. Heated micro and nano volumes of the medium experience analogous forces which can be used for pumping and mixing, for example. TW pumps and electro-thermal micro-pumps (ETμPs) are well characterized.

Keywords: electro-thermal micro-pumps, dielectrophoresis, electroorientation, electrorotation, travelling waves

1 INTRODUCTION

While micro-total analysis systems (μTAS) are employed for chemical analyses, lab-on-chip systems (LOCS) are used as *in vitro* systems for cell manipulation or culture to monitor physiological cell parameters [1, 2]. These developments aim at reducing animal testing in medical diagnostics or drug development. In the systems, microfluidic structures can be combined with integrated manipulation and sensor elements such as electrodes for the AC-electrokinetic cell or particle alignment, sorting or trapping, cell lysis, medium micropumps, as well as sensors for cell-adhesion, pH, oxygen or specific compounds. Many of the elements can be produced as platinum or indium-tin-oxide structures on glass chips, which may form the bottom plate for self-sealing microfluidic systems.

Here we focus on the various AC-electrokinetic effects which can be exploited in the chip systems [3-8]. While the observed effect depends on the field quality, the frequency dependence of the dipole moment induced in the object generates particular frequency spectra. These relations can be easily explained for DP and ER: while objects subject to DP are translated in a linear inhomogeneous field, in ER they rotate in a circular homogeneous field. The DP force and ER torque are proportional to the in-phase (mathematically the real) and out-of-phase (mathematically the imaginary) component of the induced dipole moment, respectively [3,4,9]. Combined DP and ER spectra are ideal for the dielectric characterization of single objects, because the methods permit a method-based separate access to the real and imaginary components of the induced dipole moment. Nevertheless, the AC-electrokinetic effects are not independent of each another, and combined force spectra must be expected, e.g. broken DP and ER spectra with ranges separated by the reorientation of non-spherical objects. Such spectra can be observed in combined measurements of the EO, DP and ER spectra of ellipsoidal chicken red blood cells in isotonic media of different conductivities [10]. An ellipsoidal single-shell model is the simplest possible approach for the explanation of the observed effects. For the model, the influential-radius notion allows for the separation of the geometric and electric problems and a simple description of the induced dipole moment, transmembrane potential and all AC-electrokinetic effects [3]. The size of the objects allows for an electroquasistatic description of the polarization of micro objects below 1 GHz.

2 THEORY

2.1 Polarization of objects

AC fields induce polarization charges at the structural interfaces of micro and nano objects such as particles, oil droplets, air bubbles and biological cells in suspensions or emulsions. Nevertheless, local heating may introduce "smeared interfaces" into homogeneous bulk media. Accordingly, AC-electrokinetic effects which are based on the forces generated by the interaction of the polarization charges with the inducing field can be observed with actual objects or heated micro and nano volumes of a medium.

Fig. 1 shows the two complementary cases of the effective polarization of a spherical object that may be more or less polarizable than its surrounding medium. A single-shell cell model is obtained by introducing the water droplet into a slightly larger air bubble, leaving an air film, i.e. the "biological membrane", around the droplet's surface. For low external conductivity, biological cells may qualitatively behave like water droplets (above membrane dispersion) or air bubbles (below membrane dispersion), depending on the field frequency. The interaction of these charges with the electrode charges, i.e. the external field, leads to a compression of the air bubble and an elongation of the water droplet.

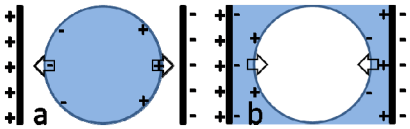

Fig. 1. Complementary AC-field polarization and force effects in air-water (representing the membranous and aqueous media in cellular systems) models while the left electrode is positively charged. Induced charges are located in water, the medium with the higher polarizability.

According to physical principles, forces are generated by potential differences, e.g. the difference between the potentials at the site of the pole in the presence and the absence of the object (Fig. 2). Please note that the effective field in confocally shelled objects polarized in a homogeneous external field is constant and corresponds to that of Maxwell's equivalent body [3, 5, 9].

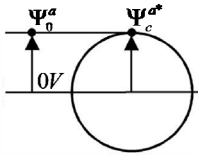

Fig. 2. Assuming the horizontal reference plane through the center of the object to be at 0 V, the vertically oriented external field (component) E_a induces the potentials $\Psi_0^a = aE_a$ in the absence and Ψ_c^{a*} in the presence of an ellipsoidal object at the site of semiaxis pole a.

Ψ_c^{a*} is highest for a vacuum object with a polarizability comparable to that of a membrane covered cell. For example, a vacuum sphere attracts the equipotential plane that is located at the "influential radius" a_{inf} distance of $3a/2$ from the symmetry plane [3, 11]. Along each semiaxis of an ellipsoidal object a_{inf}, b_{inf}, c_{inf} are the distances from the object's respective symmetry planes to those equipotential planes that just touch the respective poles of a vacuum object that has the shape of the actual object. The influential radius of semiaxis a is:

$$a_{\text{inf}} = \frac{1}{1-n_a} a \tag{1}$$

with n_a being the depolarizing factor along semiaxis a [3, 5, 9]. Please note that $n_a + n_b + n_c = 1$. While the maximum of $\Psi_c^{a*} = a_{\text{inf}} E_a$ is determined by the influential radius, i.e. the geometry of the object, its actual value is determined by the electric properties of object and suspension medium. This means that the influential-radius concept allows for the separation of the geometric and electric problems [3, 9].

Generally, the induced complex dipole moment along semiaxis a is [3, 5]:

$$m_a^* = \varepsilon_e \varepsilon_0 V f_{CM}^{a*} E_a \tag{2}$$

with n_a, $f_{CM}^{a*} = f_{CM}^{a\Re} + f_{CM}^{a\Im}$ and E_a being the depolarizing factor [3, 5], the complex Clausius-Mossotti factor consisting of its real and imaginary part and the external field component along semiaxis a.

f_{CM}^{a*} is given by the normalized potential difference at the site of pole a in the presence and absence of the ellipsoidal object (figure 2):

$$f_{CM}^{a*} = \frac{1}{n_a}\left(\frac{\Psi_0^a - \Psi_c^{a*}}{\Psi_0^a}\right) \tag{3}$$

For a single shell ellipsoid, the electric problem can be solved assuming a series circuit of three resistor-capacitor (RC) pairs for the internal, membrane and external media along each semiaxis. The impedances Z^* of the three RC pairs along a semiaxis can be calculated from the geometries of prismatic elements given by constant cross-sectional areas A and their lengths l, i.e. semiaxis length a, membrane thickness d, and length of the external medium element $a_{\text{inf}} - a$:

$$Z^* = \frac{1}{\sigma + j\omega\varepsilon\varepsilon_0} \frac{l}{A} \tag{4}$$

with $j = (-1)^{0.5}$ and $\omega = 2\pi f$, where σ, ε, ε_0, and f stand for the specific conductivity and relative permittivity of the considered medium, the permittivity of vacuum and the field frequency. The three elements form voltage-divider chains for the maximum potentials along each semiaxis thereby providing the potentials at the semiaxes poles. Along semiaxis a we obtain:

$$\Psi_c^{a*} = \frac{Z_i^{a*} + Z_m^{a*}}{Z_i^{a*} + Z_m^{a*} + Z_e^{a*}} \frac{a_{\text{inf}}}{a} \Psi_0^a \tag{5}$$

This RC model for the induced dipole moment of an oriented, ellipsoidal single-shell object can easily be extended to the general orientation and simplified for the limiting DC and very high-frequency cases as well as for certain frequency bands or dispersion processes [9]. Reduction to the membrane impedance in the nominator of the voltage-devider expression provides a general solution for the induced transmembrane voltage of ellipsoidal cells [11].

2.2 AC-electrokinetic effects

Fig. 3 gives an overview and intuitive explanations of the various AC-electrokinetic effects observed in fields induced by different electrode arrangements. Equations governing the effects can be derived from the different kinds of interaction of the induced dipole moment and the inducing field [3, 10]. In the derivation, it is assumed that small objects are polarized by a homogeneous field, i.e. the characteristic distances of the field inhomogeneity are large in comparison to the object size. At AC field frequencies beyond the hydrodynamic time constants in the system, the objects experience time-averaged effective forces and torques. Within an orthonormal coordinate system of unit vectors *i*, *j*, and *k* the ED force along semiaxis *a* is:

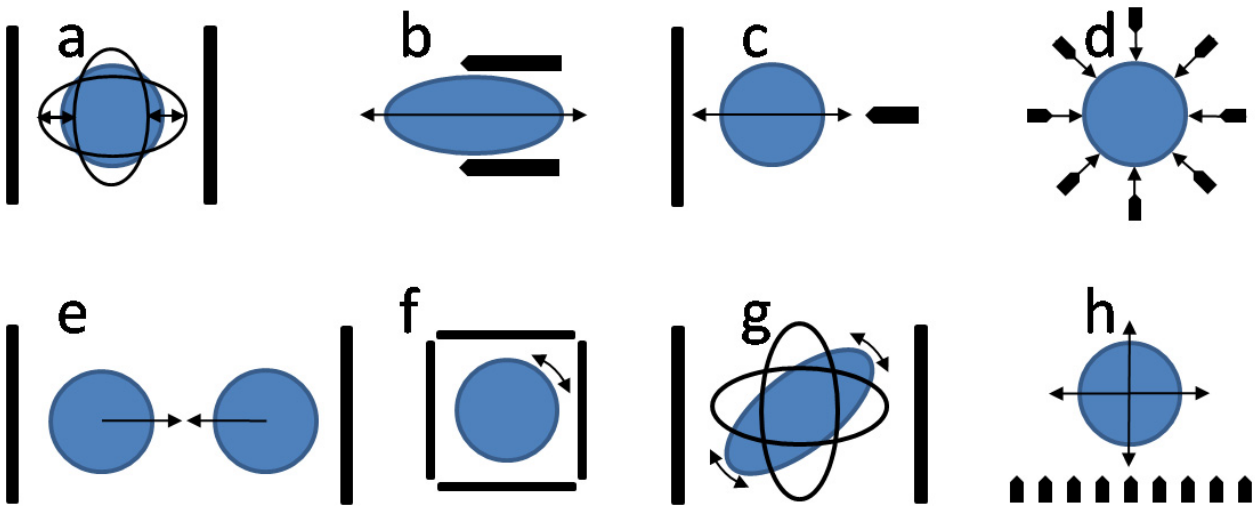

Fig. 3. Sketches of the effects observable in homogeneous (a, b, e, g), inhomogeneous (c, d), rotating (f), and TW fields (h). The field electrodes as well as the directions of forces and torques are marked by bold dark lines and arrows, respectively. (a) ED according to Fig. 1b translates into positive (elongation) or negative DP (compression) in an inhomogeneous field (c), i.e. movement of the object towards high and low field, respectively. (d) Strongly inhomogeneous fields can be used for field caging. "Inhomogeneous media" exposed to homogeneous fields experience forces that lead to pumping in ETμPs (b) or the pearl-chain formation of cells (e). (g) EO: depending on field frequency, object and medium properties, different axes of non-spherical objects will be oriented in parallel to the field. (f) At dispersion frequencies, rotating fields induce a torque leading to object rotation in or against the direction of the field. (h) This torque corresponds to the translational forces in TW DP or TW pumps with electrode arrays driven by progressively phase-shifted signals. The inhomogeneity of the field leads to vertical DP lifting or attraction.

$$\langle F_a \rangle = \varepsilon_0 \varepsilon_e E^2 f_{CM}^{a\Re} i \tag{6}$$

and the EO torque in linear or circular polarized fields is:

$$\langle N \rangle = \frac{1}{2} \varepsilon_e \varepsilon_0 V E^2 \begin{pmatrix} f_{CM}^{b\Re} & - & f_{CM}^{c\Re} \\ f_{CM}^{c\Re} & - & f_{CM}^{a\Re} \\ f_{CM}^{a\Re} & - & f_{CM}^{b\Re} \end{pmatrix} \begin{pmatrix} i \\ j \\ k \end{pmatrix} \tag{7}$$

The mutual dipole-dipole attraction over distances larger than the object size is:

$$\langle F_a \rangle = \varepsilon_0 \varepsilon_e V E^2 \left| f_{CM}^{a} \right| i \tag{8}$$

with $\left| f_{CM}^{a} \right| = \sqrt{\left| f_{CM}^{a\Re} \right|^2 + \left| f_{CM}^{a\Im} \right|^2}$. The DP and caging forces are:

$$\langle F_a \rangle = \frac{\gamma}{2} \varepsilon_0 \varepsilon_e f_{CM}^{a\Re} E^2 i \tag{9}$$

with γ describing the degree of field inhomogeneity. In ER, 4-electrodes driven by 90° phase-shifted signals are normally used to generate rotating electric fields. The dipole moment induced rotates with the same frequency, although it possesses a phase-shift with respect to the external field vector in the dispersion frequency ranges. At a given frequency, the interaction of the induced dipole moment with the external field generates a permanent torque for an ellipsoidal object rotating around its *c* axis:

$$\langle N_c \rangle = \varepsilon_0 \varepsilon_e V E^2 \frac{f_{CM}^{a\Im} + f_{CM}^{b\Im}}{2} k \tag{10}$$

Torque maxima are observed when the frequency of the exciting field is in the relaxation time ranges of the polarization along the two axes.

TWDP can be considered as a linearization of ER. The traveling effect generates a field gradient in the traveling direction of the field. For an object oriented with semiaxis a in the traveling direction of the field and an influential radius that is small in comparison to the period length $(a_{\inf} << nd)$, we obtain:

$$\langle F_a \rangle = \frac{\pi \varepsilon_0 \varepsilon_e V}{nd} E^2 f_{CM}^{a\Im} i \tag{11}$$

with *d* and *n* standing for the electrode distance and the number of electrodes for a full field period, e.g. *n*=4 for 90°-phase-shifted signals. Please note that the magnitudes of the fields, forces and torques in Eqs. 6-11 depend on how the external field is defined (for details see: [3]).

2.3 Impedance of a suspensions

The influential radius model can easily be applied to describe the impedance of suspensions of three-axial, single-shell, ellipsoidal cells or homogeneous particles using the mixing equations of Maxwell and Wagner [12]. For randomly oriented objects, the Clausius-Mossotti factors f_{CM}^{k*} (Eq. 3) along the three axes $(k = a, b, c)$ contribute by one third:

$$\frac{\sigma_S^* - \sigma_e^*}{\sigma_S^* + 2\sigma_e^*} = \frac{p}{9} \sum_{k=a,b,c} f_{CM}^{k*} \tag{12}$$

where σ^*, p and the indices S and e refer to complex specific conductivities, the volume portion of the suspended objects, the whole suspension and the external medium, respectively. Please note that the factor "1/9" in the right-hand term stems from the definition of the Clausius-Mossotti factor [12]. Eq. 12 can easily be simplified for oriented ellipsoids, spheriods or spheres.

3 CONCLUSION AND OUTLOOK

Structural polarization effects are especially suitable for the AC-electrokinetic manipulation of objects and media in LOCS for biological analysis, cell monitoring and cell culture for a number of reasons:

- The absence of moving parts.
- The effects are induced in the radio frequency range from kHz to GHz and do not interfere with optical or DC-voltage or current sensors for pH, oxygen, certain ionic species, metabolites or DNA.
- The operating frequencies avoid electrolytic processes and deterioration of metallic electrode surfaces such as gold, platinum or indium-tin oxide.
- All electric strucures can be passivated because thin layers, e.g. silicon nitrite or oxide, are capacitively bridged during operation and prevent the biological material from direct contact with metal surfaces [13].
- The parameter resolution for the object properties is higher than in impedance methods because ER, DP and EO make it possible to separately access the imaginary and real components of the induced dipole moment as well as the frequency dependence of the alterations of the axis of the maximum real component. When spectra are detected with single objects, their size, shape, orientation and internal structures can be considered in modelling [3, 9, 10].
- Caging of fluorescently labelled particles and light scattering methods such as ER-light scattering allow for the access of the dielectric properties of submicron particles [5, 7, 8].
- The driving voltages of the microstructures in LOCS correspond to standard chip voltages. Electric resonance may simply be induced by additional inductances to (locally) increase the field strength [13, 14].
- The effects of higher harmonic frequencies of rectangular driving signals can be taken into account [15].

AC-electrokinetic effects observed for objects are helpful for the intuitive understanding of the mechanisms of TWμPs or ETμPs [13]. In such pumps, the electric properties, i.e. conductivity and permittivity, of the pump media are locally altered by a temperature increase. Because no defined object interfaces exist, forces evolve from the interaction of the field with induced smeared charges in the heated volume, which are qualitatively the same as at the interfaces of objects. Similar to the relation of ED and DP, a symmetry break must be introduced for pumping, either by the channel geometry itself, by asymmetric heating (compare to Fig. 3b) or an oriented polarization by the TW field (Fig. 3h) [6, 13].

Interesting applications are possible when AC-electrokinetic effects are combined with microfluidic currents. For example the structure in Fig. 3d would be turned into a switchable filter for submicron particles or a trap for cells when located in a microfluidic channel [7, 8]. Electrode pairs at opposite walls of the microfluidic channel, protruding into the channel at an obtuse angle are able to deflect objects of certain dielectric properties by negative DP. When energized, the superposition of DP forces and fluidic shear would guide only the targeted objects to streamlines passing the end of the electrodes, thereby seperating objects of different dielectric properties. Four such electrodes could form a funnel, forming single-file object chains [17]. Finally, cells could be electrically lysed by electroporation, e.g. for genetic analysis with DNA electrodes [18].

REFERENCES

[1] P.J. Koester, S.M. Bühler, M. Stubbe, C. Tautorat, M. Niendorf, W. Baumann and J. Gimsa, Lab Chip, 10, 1579–1586, 2010.

[2] S.M. Buehler, M. Stubbe, U. Gimsa, W. Baumann and J. Gimsa, Tox. Lett., 207, 182-190, 2011.

[3] J. Gimsa, Bioelectrochem., 54, 23-31, 2001.

[4] J. Gimsa, R. Glaser and G. Fuhr, "Physical characterization of biological cells", Eds.: W. Schütt, H. Klinkmann, I. Lamprecht, T. Wilson, Verlag Gesundheit GmbH Berlin, 295-323, 1991

[5] J. Gimsa, "Electrical bio-impedance methods. Applications to medicine and biotechnology", Eds.: P.J. Riu, J. Rosell, R. Bragos, O. Casas, Ann. New York Acad. Sciences, New York, 287-298, 1999.

[6] R. Hagedorn, G. Fuhr, T. Müller and J. Gimsa, Electrophoresis, 13, 49-54, 1992.

[7] C. Reichle, T. Müller, T. Schnelle and G. Fuhr, J. Phys. D: Appl. Phys., 32, 2128–2135, 1999.

[8] G.R. Fuhr and C. Reichle, Trends Anal. Chem., 19, 402-409, 2000.

[9] J. Gimsa and D. Wachner, Biophys. J., 77, 1316-1326, 1999.

[10] S. Lippert and J. Gimsa, Proc. 2nd Int. Workshop Biol. Effects of EMFs, Ed.: P. Kostarakis, Rhodes, Greece, 830-836, 2002.

[11] J. Gimsa and D. Wachner, Biophys. J., 81, 1888-1896, 2001.

[12] K. Asami, T. Hanai and N. Koizumi, Jpn. J. Appl. Phys. 19, 359-365, 1980.

[13] M. Stubbe, A. Gyurova and J. Gimsa, Electrophoresis, 34, 562-574, 2013.

[14] J. Gimsa, T. Müller, T. Schnelle and G. Fuhr, Biophys. J., 71, 495-506, 1996.

[15] J. Gimsa, E. Donath and R. Glaser, Bioelectrochem. Bioenerg., 19, 389-396, 1988.

[16] J. Gimsa, P. Eppmann and B. Prüger, Biophys. J., 73, 3309-3316, 1997.

[17] M. Dürr, J. Kentsch, T. Müller, T. Schnelle and M. Stelzle, Electrophoresis, 24, 722–731, 2003.

[18] H. Duwensee, M. Mix, M. Stubbe, J. Gimsa, M. Adler and G.-U. Flechsig, Biosens. Bioel., 25, 400-405, 2009.

ACKNOWLEDGMENTS

The authors thank R. Sleigh for his help with the language.